

Design and Analysis of UAV

Mr. Rajdeep Gade¹, Mr. Ganesh Kadam², Mr. Chetan Jadhav³, Mr. Omkar Joshi⁴
Department of Mechanical Engineering, VIVA Institute of Technology, Virar, Mumbai, India

Abstract— The air craft making was started by Wright brothers. As before that no single aircraft was made. After so many decades every scientist got a question that many of the time in aircraft there is risk to human health to everyone started hunting solution. After so many decade scientist found a new innovation to these above problem by Remote control aircraft so this gives new born to RC aero modelling. After innovation of RC aero modelling each sectors such as military, luggage transportation, surveillance of geographical boundary was used. And now a day it is very commonly used in United States of America and in recent five years Indian government also adopting that RC aircraft culture. In India there is less awareness about RC aero modelling. Sometime model without human interface may do work which a model with human interface can't do. To utilize our knowledge about aero modelling and make a product of RC aircraft which will solve above issues. Our main aim is to lift maximum payload at minimum power consumption according to that we are designing aircraft. In every year we will planning for new & unique design for best performance. In previous year we build passenger plane and this time we are making load carrying military plane. Designed product is efficient for upcoming RC industries.

Keywords— Aero modelling, RC, Aircraft, Geographical boundary.

I. INTRODUCTION

In India RC aeromodelling in public sector is banned but in military it is used because there is no human interface so there is no risk to our soldier health. To help in military sector due to scarcity of equipments RC aeromodelling will help them while war. In India there is less awareness about RC aeromodelling. Sometime model without human interface may do work which a model with human interface can't do.

II. DESIGN LAYOUT

2.1 Optimization

2.1.1 Design Sensitivity

Sensitivity of individual components in model with respective changes and design parameter are mandatory in order to facilitate structural modifications. Wing layout is an important design variable where its span is inversely proportional to its chord length. Other variables like horizontal tail and vertical tail parameters are dependent on wing area. A secondary design variable like fuselage fineness ratio which is dependent on fuselage diameter is commonly picked between 4 and 8. This makes fuselage length dominant over fuselage diameter.

2.1.2 System of Systems

For wing, as S1223 airfoil, it has come to know that the point where S1223 gives minimum value of L/D. At point where other airfoil giving low CL, S1223 gives maximum CL. Hence airfoil is perfect for high lift.

Table 2.1.2 Selected Airfoil

Selected Airfoil -S1223					
AOA	CL	CD	CL/CD	CM	Max AOA
0	1.1864	0.01804	65.7649667	-0.2712	73.64 at $\alpha=3.75^\circ$
15	2.2502	0.06209	36.2409406	-0.1854	

For Elevator, the reason NACA 0012 airfoil is chosen is to counterbalance the moments of elevator and wing as the wing gives positive moment while S1223 helps us to get negative moment. As we compare the data of NACA 0012 and S1223 airfoils with the other airfoils, it has been seen that NACA 0012 gives convincing L/D airfoils, it has been seen that A18 gives convincing L/D ratio and S1223 gives better CL.

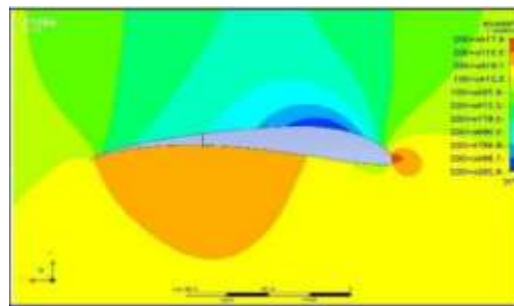


Fig.2.1.2 CFD of S1223

2.2 Drag Analysis

The 3D drag polar on an airplane is given by (from Nicolai's White paper)

$$C_d = C_{dmin} + K' C_l^2 + K'' (C_l - C_{lmin})^2$$

C_{dmin} is found by summing the contribution of each component, as calculated with equation: In this Equation,

$$C_{Dmin} = \frac{FF \times C_f \times S_{wetted}}{S_{planform}}$$

'FF' is the form factor, 'Cf' is the skin friction coefficient and can be found by using graph of Skin friction coefficient versus Reynolds Number, Sweated is the wetted surface area, and Splanform describes the planform area of the components. Below table shows these values computed at an anticipated level flight velocity of 51 feet per second. Also shown is the piecewise 3D drag contributions of each aircraft component to the overall. (Note: Reference White paper of Dr. Leland M. Nicolai, Lockheed Martin Aeronautical Company).The in viscid induced drag factor K' is calculated with Equation, Cd vs Cl Min.

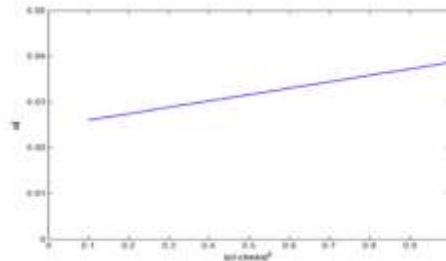


Fig. 2.2 Cd Vs Clmin

$$K' = \frac{1}{\pi A R e}$$

By the rule of thumb, we needed approximately 30W per lb-f for lifting the aircraft. Here by optimizing the performance of the aircraft, we are going to lifting the aircraft approximately 20W per lb-f of weight as we have the restriction that aircraft should be fly under 1000 Watt of power of motor & engine. The propeller which is the most important part of the aircraft which provides the required thrust to the aircraft with the help of the motor or engine. After selecting the motor the team had to select a propeller that would produce maximum thrust for our aircraft. Conforming a Slow Flyer Configuration and supporting our thesis on calculations we obtained propeller dimensions as 20 x7 inches. The selection of this propeller is done below To obtain minimum speed of our aircraft to achieve a successful takeoff and cruise flight, 135 KV motor & Zenoah G45 engine was selected. According to the data sheet provided for a selected motor the burst ampere was found out to be 85+A(180sec) and considering the current consumed by remaining control system.As per the reported KV of motor we infer battery voltage to be 22.2V 6S. The selected motor gives the enough amount of thrust at approximately 40A current. To improve the time of flight required, also maximizing the power to weight ratio charge ratings was confirmed to be 25C and 5000mAh.

$$C_D = 0.02698 + 0.07C_{l2} + 0.028(C_{l1}-0.26)^2$$

**Table 2.2
 Components Selected (with Specifications)**

Sr. no.	Component	Manufacturer	Specification	Quantity
1	B.L.D.C. motor	Cobra C-5320-22	Rpm/volt:300kv	1
2	Speed controller	Flightline 80A	Operating volt: 2-6 LiPo,80A SBEC switching	1
3	LiPo battery	ZIPPY	ZIPPY compact 6S/22.2V 5000mAh, 25C	1
4	propeller	APC electric prop	18x10 inch	1
5	Transmission And Reciever	JAPAN Remote XG7	DMSS 2 GHz Radio control system	1
6	Servo	Avionic AV55DMG	Torque speed 0.18s/60	8

III. CONSTRUCTION AND WORKING

3.1 Control System & Servo Sizing

The transmitter and receiver used in aircraft is JRXG7 (DMSS 2.4GHz). In order to ensure that the servo used to control the aircraft are of adequate size, the following calculation wa performed. The below equation gives the appropriate torque acting on ailerons, elevator and rudder.

$$T(oz - in) = 8.56 \times 10^{-6} \frac{C^2 V^2 L \sin(S1)}{\tan(S2)}$$

Above Equation generates torque values for the ailerons, elevator and rudder as 136.406oz-in, 39.322 oz-in and 25.746 oz-in respectively. The control surface length of the aileron was enough long that may cause flutter acts as cantilever. Hence team decided to use two servos of torque 138.87 oz-in on the end of surface to overcome flutter effect. The all servo used in aircraft are powered by a LIPO battery configuration 6S 5000mAh25C.

3.2 Sensitiveness Analysis

3.2.1 Constraint Diagram

It consists of poles of the sea level thrust-to-weight ratio TO/WO vs. the wing loading at take-off WO/S that are determined by various requirements set up in our intellectual pivot point.

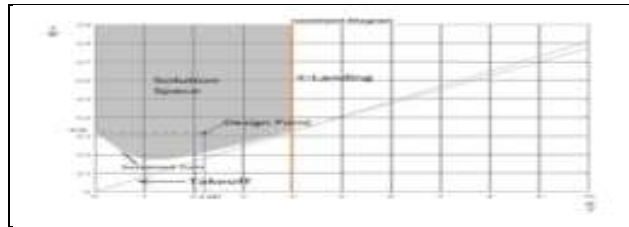


Fig. 3.2.1 Constraint Diagram

3.3. Performance Analysis

3.3.1 Runway/Launch/Landing Performance

The diagrammatic representation of takeoff and landing distance on basis of calculations explained

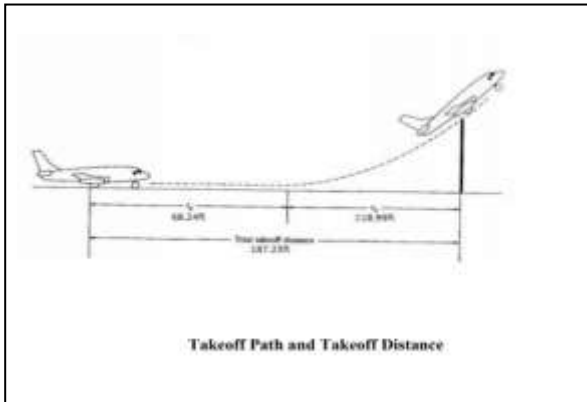


Fig.3.3.1(i) Take of path and distance

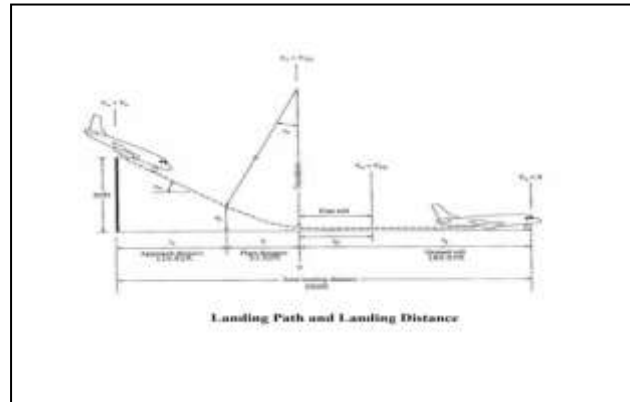


Fig.3.3.1(ii) Landing path and distance

3.2.2 Landing Constraint

If the requirements specify a maximum landing length, then landing curve represents this constraint. Values of W/s to the left of the vertical line will satisfy the constraint by resulting in a landing distance smaller than required value. So, the area to the left of landing curve is 'allowable' from the point of view of the landing constraint.

$$S_g = jN \sqrt{\frac{2W}{\rho_{\infty} S (Cl)_{max}}} + \frac{j^2 \left(\frac{W}{S}\right)}{g \rho_{\infty} (Cl)_{max} [T_{rev}/D + D/W + \mu r(1 - L/W)]}$$

3.3.1 Dynamic and Static Stability

Static margin is calculated using the formula given below.

$$\text{Static Margin} = (\text{neutral point} - \text{centre of gravity})/\text{MAC} \times 100$$

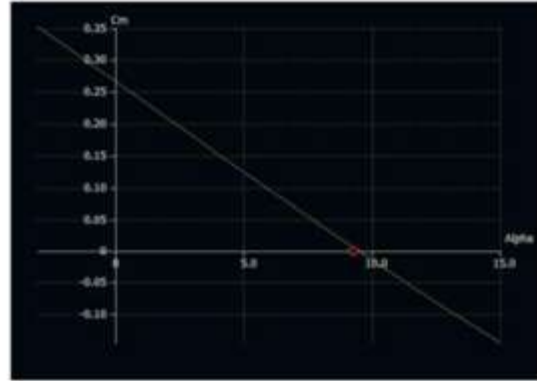
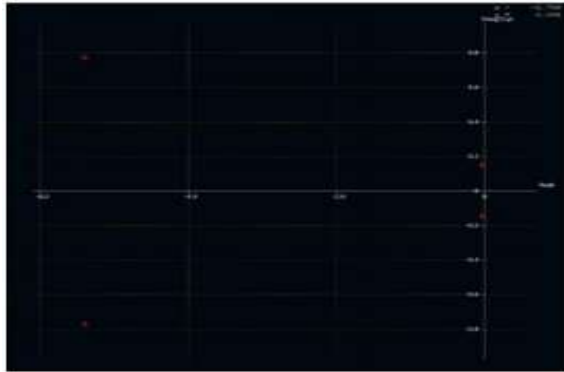
SM of our plane is 33% of MAC.

Horizontal tail and Vertical tail

Position of Horizontal Tail defines longitudinal stability whereas Vertical Tail defines directional stability of the plane. It is given by the formula,

$$\text{Horizontal tail } V_{ht} = (L_{ht} + S_{ht})/(c \times S) = 0.182$$

$$\text{Vertical tail } V_{vt} = (L_{vt} + S_{vt})/(c \times S) = 0.05$$



C_m vs. α

Fig.3.3.1 Stability Graph

IV. MANUFACTURING

Crucial feedbacks from the previous stage that gave certain change recommendations in the design were incremental in improving the state of art of the model. Of certain problems faced a few are listed in this document with practiced remedy. Human accuracy is difficult to be maintained by a small group over the course of this project. Hence all possible ribs were carved out of balsa were done so using 2-Axes CNC Laser Cutting/Engraving. This not only ensured dimensional accuracy but also high

surface finish, eliminating the need to after sanding. Not to forget that the time taken is much lesser than any human on the job. Laser cutting of parts is followed by fine sanding and identifying them by their position from CG.

Heavy Epoxy Adhesive mixture is prepared and filed syringe for high flexibility and accessibility. The airfoils and the formars are made of twin layers of aeroply to increase the strength sufficiently. The layers have been glued together in sandwich pattern using Epoxy Adhesives. Gussets have been used for making structure integrity stronger.

For mounting wing as well as motor, 5mm thick wooden plates are used as wing carries whole weight of the plane and motor causes a large amount of vibrations. Hence to absorb that vibrations, wooden plates are used as dampers. For smooth flow and to avoid drag, the leading edges of the wing, outer cage of fuselage and intersection of part assemblies have been given smooth curves. After all the parts of the body are completed, the final assembly of the aircraft takes place. This assembly is based in locknuts and blind nuts. The process marks its end with thin cover film laminating the aircraft.

V. CONCLUSION

In the conclusion we believe that this entire process of designing the aircraft compiling to strict constraints will help us grip together theoretical and practical aspects of aircraft design. It will help us to explore various specialization fields like structural Design, Computational Fluid Dynamics, and Wood Working etc.

It will not only give students a hand-on experience with hand tools as well as advanced software's but also give them an opportunity to interact with industrial tycoons in the field. Designing of aircraft would followed by rigorous quality conformance techniques which again opens new realms for students.

Testing and troubleshooting faults on ground and mid-air is as thrilling as they sound. Finally, we a group of students would learn the process of developing aircrafts from scratch, understanding various business and industrial factors.

REFERENCES

- [1] H.F. Parker, The Parker variable camber wing, Technical Report No. 77, NACA, 1920.
- [2] S. Barbarino, O. Bilgen, R.M. Ajaj, M.I. Friswell, D.J. Inman, A review of morphing aircraft, *J. Intell. Mater. Syst. Struct.* 22 (June 2011) 823–877.
- [3] E. Gillebaard, Roeland de Breuker, Optimisation of a mechanical linkage for a morphing winglet, in: *Proceedings of the DeMEASS VI Conference*, Ede, The Netherlands, May 2014.
- [4] M. Radestock, J. Riemenschneider, H.P. Monner, M. Rose, Structural optimization of an UAV leading edge with topology optimization, in: *Proceedings of the DeMEASS VI Conference*, Ede, The Netherlands, May 2014.
- [5] J. Sodja, Roeland de Breuker, M. Martinez, Geometry and force validation of the morphing leading edge concept, in: *Proceedings of the DeMEASS VI Conference*, Ede, The Netherlands, May 2014.
- [6] J.J. Joo, G.W. Reich, J.T. Westfall, Flexible skin development for morphing aircraft applications via topology optimisation, *J. Intell. Mater. Syst. Struct.* 20 (November 2009) 1969–1985.
- [7] D. Baker, M.I. Friswell, The design of morphing aerofoils using compliant mechanisms, in: *The 19th International Conference on Adaptive Structures and Technologies*, Ascona, Switzerland, October 2008. 17
- [8] P. Gamboa, J. Vale, F.J.P. Lau, A. Suleman, Optimization of a morphing wing based on coupled aerodynamic and structural constraints, *AIAA J.* 47 (9) (September 2009) 2087–2103.
- [9] B.K.S. Woods, M.I. Friswell, Preliminary investigation of a fishbone active camber concept, in: *Proceedings of the ASME 2012 Conference on Smart Materials, Adaptive Structures and Intelligent Systems*, Stone Mountain, GA, September 19–21, 2012.
- [10] B.K.S. Woods, O. Bilgen, M.I. Friswell, Wind tunnel testing of the fishbone active camber morphing concept, *J. Intell. Mater. Syst. Struct.* 25 (7) (May 2014) 772–785.